Multiple magnetic phases of $La_2CoMnO_{6-\delta}$ ($0 \leqslant \delta \leqslant 0.05$)

R. I. Dass and J. B. Goodenough
Texas Materials Institute, ETC 9.102, University of Texas at Austin, Austin, Texas 78712-1065
(Received 16 May 2002; revised manuscript received 30 August 2002; published 6 January 2003)

Transport and magnetic properties of polycrystalline $La_2CoMnO_{6-\delta}$, $0 \leqslant \delta \leqslant 0.05$, have revealed the existence of two distinguishable monoclinic ferromagnetic phases separated by a two-phase domain $0.02 \leqslant \delta \leqslant 0.05$ and a pseudotetragonal ($c/a < \sqrt{2}$) phase with $\delta \geqslant 0.05$ that was prepared at 600 °C. A nearly oxygen-stoichiometric sample having a magnetization $M(5\text{ K}, 50\text{ kOe}) = 5.78\mu_B$/f.u. with a Curie temperature $T_c \approx 226$ K is identified as atomically ordered $La_2Co^{2+}Mn^{4+}O_6$ containing about 1.8% antiferromagnetic spins at antisites. This ferromagnetic phase is an *n*-type polaronic conductor that progressively traps mobile electrons at the oxygen vacancies that introduced them on lowering the temperature. Although the x-ray-diffraction pattern can be indexed in orthorhombic (*Pbnm*) or monoclinic ($P2_1/n$) symmetry with $\beta \approx 90°$, atomic order identifies the space group as $P2_1/n$. A second monoclinic, ferromagnetic phase with $T_c < 150$ K and $\delta \approx 0.05$ has a large, positive thermoelectric power that increases progressively with decreasing temperature. Quenching a $\delta \approx 0.02$ sample from 1350 °C into liquid N_2 gave a single phase with $T_c = 134$ K and $\delta \approx 0.05$. A sample with $\delta \geqslant 0.05$ that was synthesized at 600 °C was pseudotetragonal ($c/a < \sqrt{2}$) and had a paramagnetic Weiss constant $\theta < T_c \approx 225$ K as well as a significantly smaller magnetization, but its magnetization curve $M(T)$ showed no evidence of spin-glass behavior; its large, positive thermoelectric power was characteristic of polaronic conduction without trapping of mobile charge carriers at lower temperatures. Interpretation of the two phases with $\delta \approx 0.05$ is based on the hypothesis that introduction of high-spin Mn^{3+} by the oxygen vacancies creates around it additional Mn^{3+} and intermediate-spin Co^{3+} at neighboring sites; the resulting gain in elastic energy from cooperative, dynamic Jahn-Teller deformations at these ions must be sufficient to overcome the cost of about 0.2 eV for the electron transfer from a Co^{2+} ion to a Mn^{4+} ion.

DOI: 10.1103/PhysRevB.67.014401 PACS number(s): 75.30.Cr, 75.30.Et, 75.30.Kz, 72.80.Ga

I. INTRODUCTION

The original formulation of the rules for the sign of the superexchange interactions[1,2] led to an attempt[3] to make ferromagnetic insulators by ordering Ni^{2+} and Mn^{4+} or Co^{2+} and Mn^{4+} in the double perovskites La_2NiMnO_6 and La_2CoMnO_6. Failure to achieve ordering was thought at that time to be due to an unexpected stabilization of Mn^{3+} with Ni^{3+} and Co^{3+}. A little later Blasse[4] had the same idea and attempted to prepare the same ordered compositions; but he too failed to obtain complete order although he was able to show the presence of the predicted ferromagnetic Mn^{4+}-O-Co^{2+} and Mn^{4+}-O-Ni^{2+} superexchange interactions. In those early experiments, the oxygen stoichiometry of the samples was not monitored. Recent electrochemical measurements[5] showed that the $Co^{2+} + Mn^{4+} = Co^{3+} + Mn^{3+}$ interaction is biased to the left by about 0.2 eV, and the $Ni^{2+} + Mn^{4+} = Ni^{3+} + Mn^{3+}$ interaction by about 0.8 eV. Therefore, understanding the failure to achieve full ordering of the Co^{2+} or Ni^{2+} and Mn^{4+} ions in La_2CoMnO_6 and La_2NiMnO_6 has remained a challenge. In this paper we reexamine this question and demonstrate synthesis under a high oxygen pressure of a nearly fully ordered ferromagnetic-insulator $La_2Co^{2+}Mn^{4+}O_6$ phase with a magnetization approaching $6\mu_B$ per formula unit (f.u.). We also identify a second monoclinic, ferromagnetic oxygen-deficient phase of lower Curie temperature that appears to contain at least some Co^{3+} and Mn^{3+}.

The earliest study of La_2CoMnO_6, made on samples prepared by solid-state reaction at 1300 °C in air,[3] reported the coexistence of two perovskite phases: one was *O*-orthorhombic ($a < c/\sqrt{2} < b$ in space group *Pbnm*) as distinguished from *O′*-orthorhombic ($c/\sqrt{2} < a < b$) found in the stoichiometric end member $LaMnO_3$; the other was *R*-rhombohedral $R\bar{3}c$ like the other end member $LaCoO_3$. This sample was ferromagnetic with a saturation magnetization at 4.2 K of $4\mu_B$/Mn, which led to the assumption that the sample contained high-spin Mn^{3+} and low-spin, diamagnetic Co^{3+} ions. The ferromagnetic interactions between Mn^{3+} ions were attributed to quasi-static (vibronic) superexchange interactions like those found in $LaMn_{1-x}Ga_xO_3$ where the Jahn-Teller deformations at the Mn^{3+} ions fluctuate. Chemical analysis had confirmed only Mn^{3+} in $LaMn_{1-x}Ga_xO_3$; from the total oxidizing power of La_2CoMnO_6, it was not possible to distinguish between $Mn^{3+} + Co^{3+}$ and $Mn^{4+} + Co^{2+}$. Samples prepared at 1100 °C *in vacuo* showed the presence of two distinct ferromagnetic phases with Curie temperatures of 175 and 225 K.

Blasse[4] synthesized nearly oxygen-stoichiometric La_2CoMnO_6 by solid-state reaction in air at 1000 °C followed by an anneal at 800 °C for an undisclosed period of time. From the paramagnetic susceptibility, he obtained a Curie constant $C = 4.74$ emu mol^{-1} K^{-1} ($\mu_{\text{eff}} = 6.16\mu_B$) and a Weiss constant $\theta = 270$ K, which he attributed to ferromagnetic Co^{2+}-O-Mn^{4+} superexchange interactions, but the highest measured saturation magnetization he could obtain at 4 K was only $4.82\mu_B$/f.u. Clearly atomic disorder was introducing antiferromagnetic interactions.

Recently, Joy and co-workers[6,7] prepared La_2CoMnO_6 by the low-temperature glycine-nitrate method. Samples an-

TABLE I. The synthesis conditions and room-temperature structural properties of $La_2CoMnO_{6-\delta}$ prepared under different conditions.

Sample	Synthesis conditions	Oxygen content, $6-\delta$	Space group	a (Å)	b (Å)	c (Å)	β (°)	V (Å^3)
LCM-O1	1350 °C(12 h), O_2, cool 20 °C/h	6.00(1)	$P2_1/n$	5.528(1)	7.767(1)	5.494(1)	90.01(1)	235.89(12)
LCM-O2	1350 °C(6 h), O_2, cool 180 °C/h	5.98(1)	$P2_1/n$	5.525(1)	7.770(1)	5.485(1)	90.02(1)	235.42(12)
LCM-O3	LCM-O1 at 600 °C(168 h), 3 atm. O_2, furnace cooled	6.00(1)	$P2_1/n$	5.526(1)	7.775(1)	5.492(1)	90.01(1)	235.96(12)
LCM-A1	1350 °C(16 h), air, cool 20 °C/h	5.98(1)	$P2_1/n$	5.524(1)	7.763(1)	5.487(1)	90.01(1)	235.30(12)
LCM-Q1	LCM-A1 at 1350 °C(3 h), air, quenched in liquid N_2	5.95(1)	$P2_1/n$	5.522(1)	7.764(1)	5.480(1)	90.01(1)	234.99(12)
LCM-AR1	1350 °C(8 h), Ar, cool 180 °C/h	5.95(1)	$P2_1/n$	5.524(1)	7.768(1)	5.482(1)	90.01(1)	235.24(12)
LCM-LT1	600 °C(12 h), air, cool 180 °C/h	$\leqslant 5.95$	Pseudotetragonal	5.518(2)		7.766(3)		236.46(26)

nealed at 700 °C in air were reported to be rhombohedral with a well-defined $T_c = 225$ K; the paramagnetic susceptibility gave a $\mu_{\text{eff}} = 3.52\mu_B$ and a $\theta = 378$ K as extrapolated from above 600 K. On the other hand, samples annealed at 1300 °C in air had orthorhombic symmetry with a $T_c = 150$ K, a $\mu_{\text{eff}} = 4.01\mu_B$, and $\theta = 236$ K as extrapolated from above 450 K. They interpreted these findings to represent high-spin Mn^{3+} and low-spin Co^{3+} in the rhombohedral phase and high-spin Co^{2+} and Mn^{4+} in the orthorhombic phase. Samples prepared in the range $700\,°C < T < 1300\,°C$ contained both phases. Neither the saturation magnetization at 4 K nor the oxygen stoichiometry of their two phases were reported. Jonker[8] reported a maximum in the resistivity of the system $LaCo_{1-x}Mn_xO_3$ near $x = 0.5$, which is consistent with Co^{2+} and Mn^{4+} ions in samples with $x = 0.5$.

The present work had four objectives: (1) to clarify the different chemistries and structures of the two magnetically distinguishable phases, (2) to determine the origin of the phase segregation, (3) to synthesize a single-phase ferromagnetic insulator having ordered Co^{2+} and Mn^{4+} ions, and (4) to investigate whether the ordered phase contained antiphase boundaries between ordered domains.

II. EXPERIMENTAL PROCEDURES AND RESULTS

A. Synthesis

$La_2CoMnO_{6-\delta}$ was synthesized by the Pechini method[9] with $La(NO_3)_3 \cdot 6.03(1)H_2O$, $Co(NO_3)_2 \cdot 5.94(1)H_2O$, and $Mn(CH_3COO)_2 \cdot 3.54(1)H_2O$ as the starting materials. The water of crystallization of the salts was determined by thermogravimetric analysis (TGA) with a heating rate of 1 °C/min in flowing air for the nitrates and in a flowing mixture of 5% H_2/Ar for the acetate. Stoichiometric quantities of the salts were dissolved in deionized water; a little dilute nitric acid was added to ensure complete dissolution of the acetate. Citric acid was then added to the stirring red solution; 1 mol per 1 mol of trivalent cation and $\frac{2}{3}$ mol per 1 mol of divalent cation were required. In this synthesis, 1.5 times the stoichiometric amount of citric acid was needed to complete the chelation. After 30 min of stirring, the same molar volume of ethylene glycol as citric acid was added to the pink chelated solution. The solution was then heated to approximately 150 °C to allow the chelates to undergo polyesterification as well as to remove excess water. The resulting dark-brown gel was completely dried in an oven, ground, and slowly decomposed in air at 375 °C for 24 h. The product, a dark-brown powder, was ground, pressed into half-inch-diameter pellets 2–5 mm thick, and annealed in different flowing atmospheres at the temperatures and for the times indicated in Table I. With one exception, sample LCM-Q1, all samples were cooled to room temperature in their respective atmospheres at the cooling rates also indicated in Table I. Sample LCM-Q1 was obtained by quenching LCM-A1 into liquid N_2 after annealing for 3 h at 1350 °C in air. Note that LCM-O3 was produced by sintering sample LCM-O1 at 600 °C in 3 atm of O_2 for seven days and furnace cooling to room temperature. All samples synthesized at $T \leqslant 700\,°C$ were black and soft while those sintered at 1350 °C were greenish-gray and very dense.

The oxygen stoichiometry, the $6-\delta$ of Table I, of all the samples was determined by complete reduction in flowing 5% H_2/Ar to a mixture of La_2O_3, MnO, and Co metal in a Perkin-Elmer Series 7 Thermogravimetric Analyzer (TGA) at a heating rate of 1 °C/min to 1000 °C. A typical TGA plot is shown in Fig. 1. The oxygen stoichiometry of all samples annealed at 1350 °C was reproducible; the variation from sample to sample fell within the range $0 \leqslant \delta \leqslant 0.05$. The δ for samples sintered at $T \leqslant 700\,°C$ was difficult to resolve because of adsorbed water on the large surface area of the powders. From Table I, it appears that the oxygen stoichiometry is governed not only by the synthesis temperature and oxygen partial pressure, but also by the rate at which the sample is cooled.

B. Structure

The identification of all phases and determination of room-temperature lattice parameters were accomplished with a Philips PW 1729 powder x-ray diffractometer equipped with a pyrolytic graphite monochromator and Cu $K\alpha$ radiation ($\lambda = 1.54059$ Å); KCl was the internal standard. Data were collected in steps of 0.020° over the range $10° \leqslant 2\theta \leqslant 100°$ with a count time of 15 s per step. Peak profiles were fitted with the program JADE, and lattice parameters were refined by a least-square method developed by Novak and Colville.[10] The lattice constants of the different samples are also given in Table I.

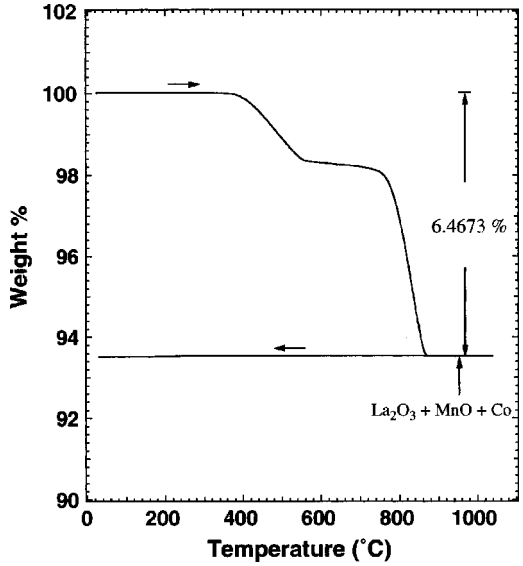

FIG. 1. The TGA plot of LCM-A1 (1350 °C, air, 16 h, cool 20 °C/h) in a flowing atmosphere of 5% H_2/Ar.

All samples were single-phase to x-ray diffraction. Due to the small difference in scattering factors of Co and Mn,[11] no superstructure lines were observed. All samples that had been heated to 1350 °C were highly crystalline with narrow x-ray-diffraction peaks, e.g., Fig. 2, that were easily refined within two possible space groups, orthorhombic *Pbnm* ($Z=2$) and monoclinic $P2_1/n$ ($Z=2$) with a $\beta \approx 90°$. The former corresponds to a random distribution of Co and Mn over the octahedral sites of the perovskite structure, the latter to an ordering of Co^{2+} and Mn^{4+} ions into distinguishable $2c$ and $2d$ sites. Discrimination between these alternatives in favor of the monoclinic phase comes from a consideration of the magnetic properties as is discussed below.

Table I shows a nearly constant a parameter and $\beta \approx 90°$ for all samples indexed as monoclinic $P2_1/n$. The stoichiometric sample LCM-O3, which was annealed under 3 atm O_2 at 600 °C, had the largest cell volume. The volume decreased as the oxygen deficit δ increased.

In an attempt to duplicate the low-temperature phase indexed by Joy and co-workers[6,7] as *R*-rhombohedral, we sintered in air at 600 °C the dark-brown powder formed at 375 °C for 12 h followed by cooling to room temperature at a rate of 180 °C/h. The poorly crystalline black powder gave broad diffraction peaks (Fig. 2) that could not be indexed in rhombohedral $R\bar{3}c$ symmetry, but could be refined within a pseudotetragonal model with $a=b\approx\sqrt{2}a_p$ and $c\approx 2a_p$, where $a_p \approx 3.90$ Å is the lattice parameter for a cubic perovskite. A $c/\sqrt{2} < a=b$ shows that this phase does not contain a cooperative twisting of the octahedra about the *c*-axis as occurs in low-temperature $SrTiO_3$. The x-ray diffraction peaks of Joy *et al.*[7] for the low-temperature phase were too broad to allow an unambiguous crystal-symmetry assignment.

The LCM-O3 sample was the product of an attempt to synthesize a more crystalline low-temperature phase. We did not convert the monoclinic phase to either a rhombohedral or a tetragonal phase by annealing the LCM-O1 phase at 600 °C under 3 atm O_2, but we did succeed in approaching closer to oxygen stoichiometry in the monoclinic phase as judged by the increase in volume.

C. Thermoelectric power

For all samples, the Seebeck coefficient $\alpha(T)$, Fig. 3, was obtained with a laboratory-built apparatus as described elsewhere.[12] Since all the samples were polaronic conductors of high resistivity below 300 K, the data became unreliable below 150 K due to the impedance limits of the apparatus. A correction was applied to compensate for the small contribution to $\alpha(T)$ from the leads.

The inset of Fig. 3 shows a large, negative $\alpha(T)$ for the two oxygen-stoichiometric samples LCM-O1 and LCM-O3; the increase in the magnitude of $\alpha(T)$ with decreasing temperature signals a progressive trapping out or annihilation of *n*-type polarons as the temperature is lowered. Surprisingly,

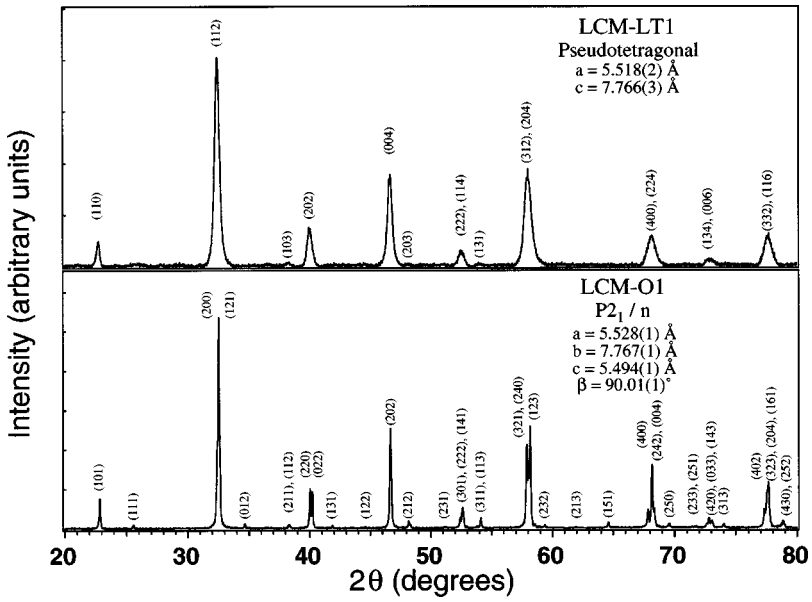

FIG. 2. The room-temperature powder x-ray-diffraction patterns of pseudotetragonal LCM-LT1 (600 °C, air, 12 h, cool 180 °C/h) and monoclinic LCM-O1 (1350 °C, O_2, 12 h, cool 20 °C/h).

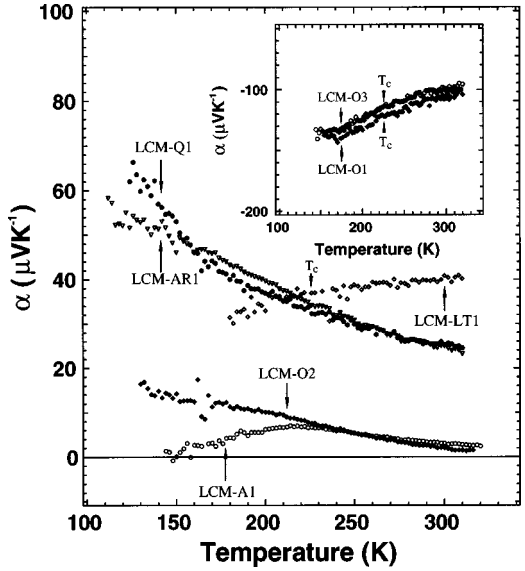

FIG. 3. The variation of the thermoelectric power $\alpha(T)$ for all compositions in the system $La_2CoMnO_{6-\delta}$ ($0 \leqslant \delta \leqslant 0.05$). The ferromagnetic Curie temperature T_c is indicated for some of the compositions.

the most oxygen-deficient samples LCM-Q1 and LCM-AR1, each with $\delta \approx 0.05(1)$, exhibit a large, positive $\alpha(T)$ that increases on lowering the temperature even though an oxygen deficiency can be expected to introduce electrons, not holes, into the $CoMnO_{6-\delta}$ array. The samples LCM-O2 and LCM-A1, with $\delta \approx 0.02(1)$, show an intermediate magnitude and temperature dependence of $\alpha(T)$.

D. Magnetic data

Magnetic data for all samples of this study were taken with a Quantum Design dc superconducting quantum interference device (SQUID) magnetometer; the results are summarized in Table II. Figure 4 shows magnetization M versus

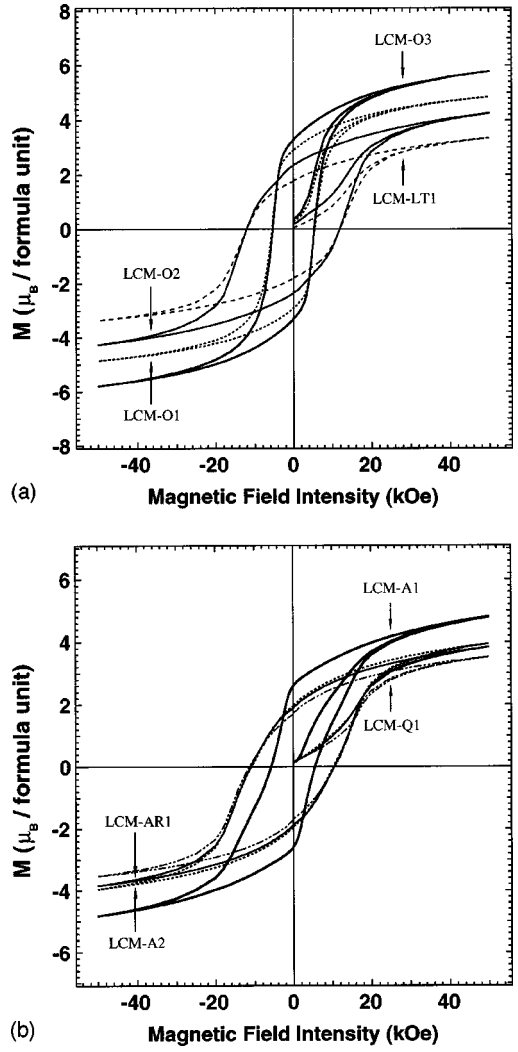

FIG. 4. The *M-H* hysteresis loops of all compositions in the system $La_2CoMnO_{6-\delta}$ ($0 \leqslant \delta \leqslant 0.05$) at $T = 5$ K.

TABLE II. The magnetic properties of $La_2CoMnO_{6-\delta}$ ($0 \leqslant \delta \leqslant 0.05$) prepared under different conditions. *F* refers to ferromagnetism and T_{ci} is the Curie temperature of long-range ferromagnetic order. M(50 kOe), M_r, and H_{ci} are the magnetization at 50 kOe, the remanent magnetization, and the coercivity, respectively,

Sample	Type of magnetic behavior	Magnetic transition temperature (K)	M(5 K, 50 kOe) (μ_B/f.u.)	M_r (5 K) (μ_B/f.u.)	H_{ci} (5 K) (Oe)	$\mu_{\text{eff}}(\mu_B)$	θ (K)
LCM-O1	*F*	$T_c = 226(2)$	4.85(2)	2.90(2)	5520(10)	5.96(2)	300(2)
LCM-O2	*F*	$T_{c1} = 180(2)$	4.26(2)	2.35(2)	12100(20)	5.92(2)	268(2)
LCM-O3	*F*	$T_c = 226(2)$	5.78(2)	3.30(2)	5350(10)	6.00(1)	298(2)
LCM-A1	*F*	$T_{c1} = 212(2)$	4.82(2)	2.58(2)	5700(10)	5.93(2)	274(2)
LCM-A2	*F*	$T_{c1} = 208(2)$	3.95(2)	1.95(2)	10700(20)		
	F	$T_{c2} = 148(2)$					
LCM-Q1	*F*	$T_c = 134(2)$	3.53(2)	1.69(2)	11280(20)	5.93(2)	236(2)
LCM-AR1	*F*	$T_{c1} = 202(2)$	3.83(2)	1.88(2)	10900(20)	5.99(2)	244(2)
	F	$T_{c2} = 148(2)$					
LCM-LT1	*F*	$T_c = 225(2)$	3.36(2)	1.78(2)	12080(20)	5.85(2)	212(2)

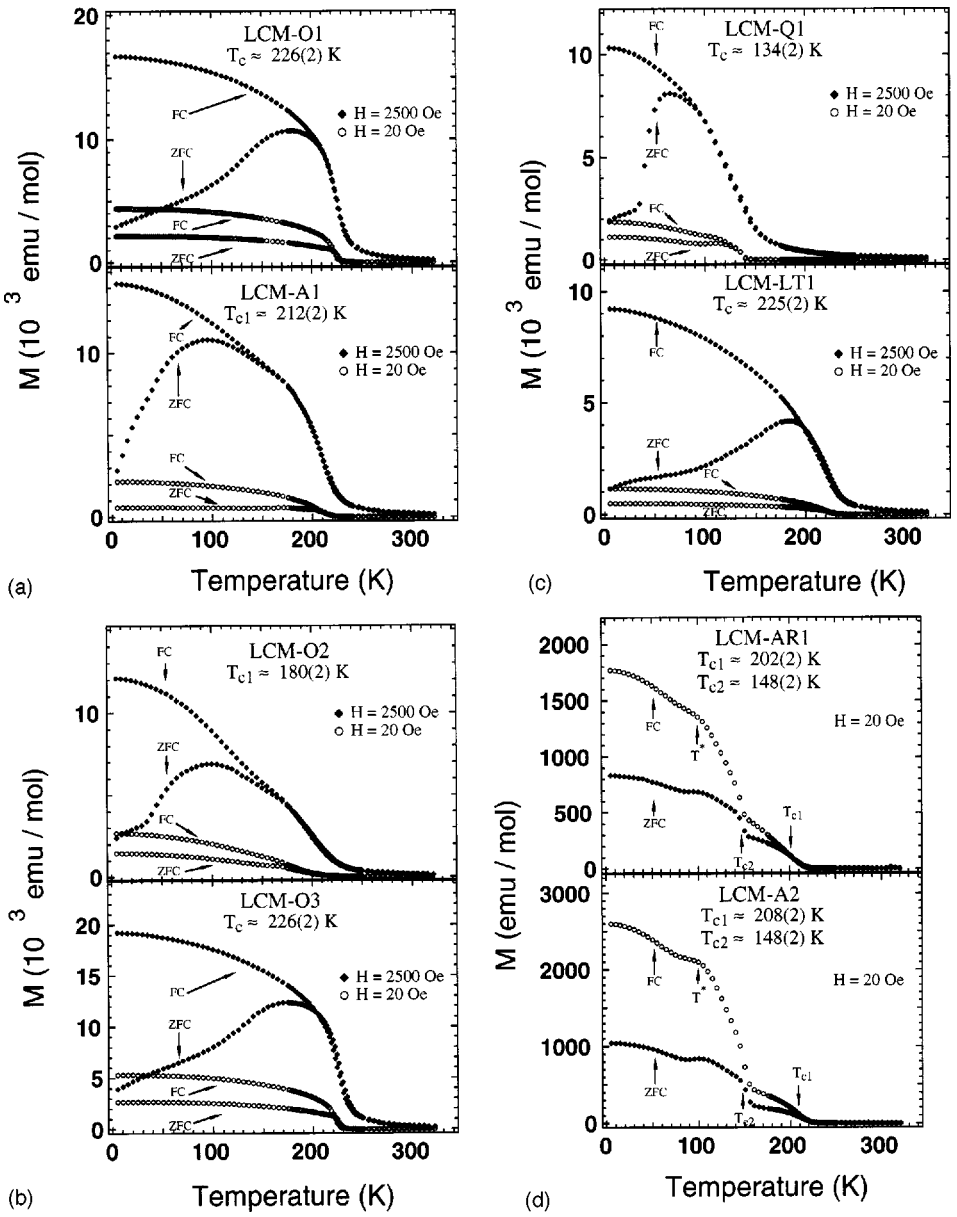

FIG. 5. The temperature dependence of the molar magnetization M under different applied fields H for all compositions in the system $La_2CoMnO_{6-\delta}$ ($0 \leqslant \delta \leqslant 0.05$). The ferromagnetic Curie temperature T_c is indicated for some of the compositions.

applied magnetic field H obtained at 5 K over the range -50 kOe$\leqslant H \leqslant$50 kOe; they provide the M(5 K, 50 kOe), the coercivity H_{ci}(5 K), and the remanance M_r(5 K) of Table II. Figure 5 shows $M(T)$ curves taken on cooling in fields of 20 and 2500 Oe [field cooling (FC)] and on heating in these same fields after cooling in zero field (ZFC). The Curie temperatures T_c of Table II were taken from the inflection point of the low-field data. The existence of a ferromagnetic phase with $T_c = 134$ K was found in the quenched sample LCM-Q1 having a $\delta \approx 0.05(1)$, and it can be seen in the 20-Oe $M(T)$ curve to be the dominant phase in sample LCM-AR1, also having a $\delta \approx 0.05(1)$. In order to determine whether the difference in behavior between these two $\delta \approx 0.05(1)$ samples can be attributed to clustering of the oxygen vacancies, sample LCM-$A2$ was synthesized by annealing in air at 1350 °C for 16 h the dark-brown powder formed at 375 °C; this sample was cooled at 180 °C/h to room temperature, and TGA analysis gave it a $\delta \approx 0.04(1)$, a little smaller than that of LCM-Q1 and LCM-AR1. The $M(T)$ curve at 20 Oe for this crystallographically single-phase sample is also shown in Fig. 5. Paramagnetic molar susceptibilities $\chi_{\rm mol}$ were taken over the range 300 K$\leqslant T \leqslant$700 K; from the straight-line portion of $\chi_{\rm mol}^{-1}$ of Fig. 6, we obtained the values of the $\mu_{\rm eff}$ in μ_B and the Weiss constant θ shown in Table II.

III. DISCUSSION

Since these compounds are all insulators, double exchange is not a factor, and interpretation of these results begins with the rules for the sign of the spin-spin superexchange interactions: (1) half-filled to empty orbital virtual spin transfer as in e^2-O-e^0, ferromagnetic coupling; (2) half-filled to half-filled orbital virtual charge transfer as in e^2-O-e^2 or t^3-O-t^3, antiferromagnetic coupling. In addition, (3) interactions via σ-bonding e orbitals dominate those by

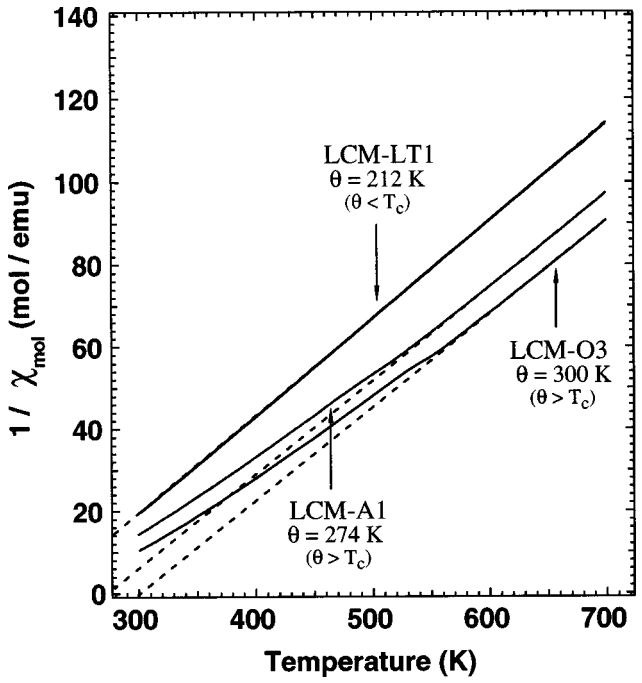

FIG. 6. The variation of the paramagnetic inverse molar susceptibility χ_{mol}^{-1} with temperature for some compositions of the system $La_2CoMnO_{6-\delta}$ ($0 \leqslant \delta \leqslant 0.05$) in $H = 50$ kOe. The dashed lines are guides for the eye.

π-bonding t orbitals where both are present in the same total interaction, and (4) Jahn-Teller ions having a single electron in twofold-degenerate, fluctuating e-orbital occupation as in e^1-O-e^1 give a three-dimensional ferromagnetic, vibronic superexchange interaction.[13,14] Ordering of Mn^{4+} and Co^{2+} ions in $La_2Co^{2+}Mn^{4+}O_6$ gives ferromagnetic e^2-O-e^0 interactions, but point disorder creates antiferromagnetic Mn^{4+}-O-Mn^{4+} or Co^{2+}-O-Co^{2+} interactions with the antisite ions. Moreover, in an ordered double perovskite, nucleation of atomic order at different positions results in antiphase boundaries if the positions of the Co^{2+} and Mn^{4+} are inverted in one ordered region relative to that in a neighboring region. The antiphase interface between the two regions would have antiferromagnetic Co^{2+}-O-Co^{2+} or Mn^{4+}-O-Mn^{4+} interactions, whereas both ordered regions would have ferromagnetic Co^{2+}-O-Mn^{4+} interactions. Antiparallel coupling of the neighboring domains gives a low remanent magnetization M_r, but in an external magnetic field $H = 50$ kOe, all the ferromagnetic regions become aligned with only a 360° domain wall residing at the antiphase boundary.[15] Finally, we note that local Jahn-Teller deformations can stabilize intermediate-spin Co^{3+}:t^5e^1,[16,17] and transfer of an e electron from a Co^{2+} to a Mn^{4+} would create intermediate-spin Co^{3+} and high-spin Mn^{3+}. Such a transfer across a 0.2 eV gap would only occur, if at all, in regions about a Mn^{3+} ion in a reduced $La_2CoMnO_{6-\delta}$ so as to reduce the elastic energy associated with local occupied-e-orbital fluctuations by introducing *cooperative* local Jahn-Teller deformations.[18] With this background, we turn to the experimental results.

The LCM-O3 phase with $T_c = 226$ K is the most nearly oxygen stoichiometric and has an $M(5\text{ K}, 50\text{ kOe}) = 5.78\mu_B$/f.u., which approaches the spin-only $6\mu_B$/f.u. for both fully ordered $La_2Co^{2+}Mn^{4+}O_6$ and disordered $La_2Co^{3+}Mn^{3+}O_6$. This is the highest magnetization for this compound that has ever been reported. Since it is nearly oxygen stoichiometric, we may assume that this phase is ordered $La_2Co^{2+}Mn^{4+}O_6$ with about 1.8% antisite Co^{2+} and Mn^{4+}, i.e., with an order parameter that approaches unity. A field of 50 kOe is sufficient to orient any antiparallel antiphase regions parallel to their neighbor parallel regions with only a 360° domain wall at the antiphase boundary.[15] However, 50 kOe is not sufficient to reorient the antiferromagnetic spins at point antisite ions. At $H = 0$, any antiphase regions would revert back to an antiparallel orientation with a 180° change of spin orientation across an antiphase boundary, which would lower the remanent magnetization M_r. The fact that $M_r = 3.30\mu_B$/f.u. in this polycrystalline sample indicates that there are few, if any, antiphase regions in the LCM-O3 sample. Moreover, failure to reach full saturation by 50 kOe could be due to canting of the antisite spins as well as to a large crystalline anisotropy of the octahedral-site Co^{2+} ions. In the double perovskite Sr_2FeMoO_6, the antiferromagnetic coupling across antiphase boundaries lowers M_r to an extremely small value.[15]

The LCM-O1 sample contains a few more oxygen vacancies than LCM-O3, and the Co^{2+} and Mn^{4+} ions are not so well ordered. Nevertheless, both the LCM-O1 and LCM-O3 samples have a paramagnetic Weiss constant $\theta > T_c$ characteristic of ferromagnetism as opposed to ferrimagnetism.

Sample LCM-Q1 with $\delta = 0.05(1)$ has an $M(T)$ curve showing a single ferromagnetic phase with $T_c = 134$ K whereas the unquenched samples LCM-AR1 and LCM-A2 with $\delta = 0.05(1)$ and $\delta = 0.04(1)$, respectively, each have $M(T)$ curves showing a minority ferromagnetic phase with $T_{c1} = 202$ and 208 K, respectively, and a majority ferromagnetic phase with $T_{c2} = 148$ K. Samples LCM-O2 and LCM-A1, each with an oxygen deficiency $\delta = 0.02(1)$, also exhibit an $M(T)$ curve in 2500 Oe that deviates from a Brillouin function; its shape is characteristic of the coexistence of two ferromagnetic phases, one with a $T_{c1} = 180$ and 212 K, respectively, and the other with a $T_{c2} < 150$ K. Thus a two-phase region between two distinguishable ferromagnetic phases is seen to span the range $0.02 \leqslant \delta \leqslant 0.05$ with stabilization of a single $\delta = 0.05(1)$ phase on quenching from 1350 °C. Although a first-order phase change distinguishes the oxygen-deficient phase having $T_{c2} < 150$ K from the oxygen-stoichiometric phase having a $T_{c1} = 226$ K, nevertheless, synthetic conditions that do not allow segregation to go to thermodynamic equilibrium in the two-phase region causes T_{c1} to be lowered from 226 K and T_{c2} to be raised from 134 K.

The Seebeck $\alpha(T)$ data of Fig. 3 are unusual and informative. The nearly oxygen-stoichiometric samples LCM-O3 and LCM-O1 with $T_c = 226$ K have a negative $\alpha(T)$ that increases in magnitude on cooling from room temperature whereas samples LCM-Q1 and LCM-AR1 in which the high-T_c phase is either absent or present in too low a concentration to percolate have a positive $\alpha(T)$ that increases

with decreasing temperature. Samples LCM-O2 and LCM-A1 contain contributions to $\alpha(T)$ from both phases and therefore have intermediate values of $\alpha(T)$. The magnitudes and temperature dependencies of the single-phase samples are typical of low-concentration polaronic conduction with a progressive trapping out of mobile charge carriers as the temperature is lowered.

A negative $\alpha(T)$ of large magnitude for the nearly oxygen-stoichiometric samples LCM-O3 and LCM-O1 (inset of Fig. 3) is consistent with a small concentration of oxygen vacancies that attract the Mn^{3+} ions they introduce; fivefold oxygen coordination at Mn^{3+} ions bordering on oxygen vacancy has been well established.[19] Thermal excitation of an e^1 electron at a trapped Mn^{3+} to a Mn^{4+} ion not bordering a vacancy would give *n*-type polaronic conduction on the Mn subarray. If an oxygen vacancy traps two Mn^{3+} ions, one of them must be in an antisite; in this way, oxygen vacancies would contribute to atomic disorder. However, if the oxygen vacancy does not perturb the atomic ordering, it can only trap one of the two Mn^{3+} ions it introduces.

The appearance of *p*-type conductivity in the low-T_{c2} phase having $\delta \approx 0.05(1)$ is remarkable since reduction introduces Mn^{3+} ions. The mobile Mn^{3+} ions introduced by oxygen vacancies would have their *e* electrons strongly coupled to fluctuating, local Jahn-Teller distortions of their octahedral sites. If these distortions were to induce transfer of an *e* electron from the Co^{2+} ions to neighboring Mn^{4+} ions, creating intermediate-spin Co^{3+} and Mn^{3+} ions, in order to gain elastic energy by making the local Jahn-Teller distortions cooperative, a vibronic majority-spin σ^* band of *e*-electron parentage would be created and would be more than half-filled so as to give a positive thermoelectric power $\alpha(T)$. However, the large magnitude of $\alpha(T)$ and its increase with decreasing temperature show that this simple picture is inadequate. The mobile charge carriers must be confined to a subset of the transition-metal atoms; regions of ordered Co^{2+} and Mn^{4+} would not carry the mobile charge carriers. Trapping out of Mn^{3+} either as Co^{2+} and Mn^{4+} in the ordered regions or in static orbitally ordered clusters on lowering the temperature could further reduce the number of atomic sites on which the charge carriers travel, thus reducing the hole concentration in the vibronic σ^* orbitals of the conductive volume and raising $\alpha(T)$.

Although we do not make a calculation to justify the assumption that the elastic energy gained by a cooperative Jahn-Teller distortion could be sufficient to induce the transfer of an *e*-electron from a Co^{2+} to a Mn^{4+} ion across a 0.2-eV energy gap, we can point to evidence that the gain in elastic energy is sufficient to induce chemical heterogeneity in a single-phase spinel. Some years ago, the elastic energy gained by a cooperative dynamic Jahn-Teller distortion between Mn^{3+} ions was identified as the driving force to create Mn-rich inhomogeneities responsible for the realization of a square *B-H* hysteresis loop in polycrystalline ferrite memory cores.[18] We are suggesting here that this energy gain is sufficient to bias the reaction $Co^{2+} + Mn^{4+} = Co^{3+} + Mn^{3+}$ to the right in a small, but finite, volume about an isolated Mn^{3+} ion introduced by oxygen vacancies. The volume in which electron transfer occurs would be greater at higher temperatures; it would inhibit long-range ordering of Co and Mn on different lattice sites, stabilizing instead vibronic, ferromagnetic superexchange interactions in an atomically disordered volume. Since vibronic superexchange would give a smaller stabilization than a static ferromagnetic superexchange, a vibronic ferromagnetic Curie temperature would be lower than that of the ordered $La_2Co^{2+}Mn^{4+}O_6$ phase.

Support for this model comes from the LCM-LT1 phase, which presents another puzzle. The LCM-LT1 phase has the $T_c = 225$ K of the high-T_{c1} phase, but a low value of M(5 K, 50 kOe) and a $\theta < T_c$ differentiates it from the ferromagnetic LCM-O3 phase. Moreover, a pseudotetragonal structure with $c/a < \sqrt{2}$ is not compatible with cooperative rotations of octahedra about the *c*-axis, but it is compatible with a static ordering of occupied e^1 orbitals as occurs in the O'-orthorhombic ($c/a < \sqrt{2}$) structure of $LaMnO_3$, which also has a $\theta \leqslant T_c$. $LaMnO_3$ has a canted-spin ferromagnetic component of its antiferromagnetically coupled, ferromagnetic (001) planes. A static, cooperative ordering of occupied e^1 orbitals requires a significant concentration of Jahn-Teller ions; therefore stabilization of intermediate-spin Co^{3+} and Mn^{3+} versus Co^{2+} and Mn^{4+} in a percolating matrix is required if the crystallographic distortions is due to a cooperative Jahn-Teller orbital ordering. This sample, prepared at 600 °C, is oxygen deficient with $\delta \geqslant 0.05$, so whatever model is proposed should relate to that for the ferromagnetic oxygen-deficient phase with $T_{c2} = 135$ K. In that model, we proposed a percolating volume of intermediate-spin Co^{3+} and Mn^{3+} ions that retains fluctuating Jahn-Teller deformations. An LCM-LT1 phase would be formed if the volume of fluctuating Jahn-Teller deformations transformed to a long-range, static cooperative Jahn-Teller deformation as occurs in $LaMnO_3$ below 750 K. Such a model would introduce the coexistence of an atomically disordered, but orbitally ordered phase having antiferromagnetic Mn^{3+}-O-Mn^{3+} interactions in one direction coexisting with an atomically ordered ferromagnetic phase and could therefore account for a single high-T_{c1} Curie temperature and a reduced magnetization. On the other hand, there is no evidence of spin-glass behavior, and the positive $\alpha(T)$ has a temperature dependence typical of a polaronic conductor without a progressive trapping out of the mobile polarons on lowering the temperature. However, this situation would be found if the atomically disordered phase underwent a static orbital ordering in only part of its volume and interfaced the ferromagnetic phase with its ferromagnetic (001) planes; a vibronic atomically disordered transitional layer containing mobile charge carriers would interface the atomically ordered ferromagnetic phase. Since both the orbitally ordered and atomically ordered volumes percolate, the orbitally fluctuating interface layer would also and would give the observed $\alpha(T) > 0$.

IV. SUMMARY AND CONCLUSIONS

This study has clarified the different chemistries and structures of not two, but three thermodynamically distinguishable phases. We have managed to synthesize a ferromagnetic $La_2Co^{2+}Mn^{4+}O_6$ double perovskite with a nearly complete ordering of the Co^{2+} and Mn^{4+} ions by oxidizing

nearly all the Mn to Mn^{4+} in a nearly oxygen-stoichiometric sample. Oxygen vacancies introduce Mn^{3+} ions and tend to trap a second Mn^{3+} near neighbor in an antisite position, thus lowering the atomic order and the saturation magnetization. Electrons excited from trapped Mn^{3+} or, if a second Mn^{3+} was not attracted as a near neighbor, donated as mobile electrons on the Mn subarray give *n*-type polaronic conduction. The most nearly oxygen stoichiometric sample had a magnetization at 5 K in 50 kOe as high as $M(5\text{ K}, 50\text{ kOe}) = 5.78\mu_B$/f.u. and a $T_c = 226$ K. The atomically ordered matrix contains distinguishable Co^{2+} and Mn^{4+} sites, which classifies the space group as monoclinic $P2_1/n$ with $\beta \approx 90°$ rather than orthorhombic *Pbnm*. Atomic disorder introduces clusters containing antiferromagnetic Mn^{4+}-O-Mn^{4+} or Co^{2+}-O-Co^{2+} interactions that align the antisite spins antiferromagnetic with respect to the ferromagnetic matrix. Antiferromagnetic interactions across antiphase boundaries would introduce antiferromagnetically coupled ferromagnetic volumes with a 180° spin reversal pinned in an external field $H = 0$ at the antiphase boundary. A field $H = 50$ kOe is large enough to align the volumes, creating a 360° domain wall at the antiphase boundary. Normally, such a situation leads to a *B-H* hysteresis loop with a very small remanence whereas the ordered $La_2Co^{2+}Mn^{4+}O_6$ sample had a remanent magnetization $M_r = 3.3\mu_B$/f.u. Failure to obtain a saturation magnetization of $6\mu_B$/f.u. appears to be due to atomic disorder primarily associated with oxygen vacancies rather than to the presence of antiphase boundaries.

A second ferromagnetic phase with a $T_c = 134$ K was found in a $La_2CoMnO_{6-\delta}$ sample with $\delta = 0.05(1)$ that had been quenched from 1350 °C into liquid N_2. If the Co and Mn are disordered in this phase, it is to be classified orthorhombic *Pbnm*. Although this perovskite is reduced, it has polaronic conduction with a positive thermoelectric power and the charge carriers are progressively trapped out with decreasing temperature. The positive thermoelectric power can be understood if the mobile charge carriers occupy a vibronic σ^* band associated with an atomically disordered volume containing intermediate-spin Co^{3+} and Mn^{3+}; vibronic e^1-*O*-e^1 superexchange would give a three-dimensional ferromagnetic coupling, but with a smaller exchange stabilization than the Co^{2+}-O-Mn^{4+} interactions of the atomically ordered phase and therefore a lower T_c. Since the transfer of an electron from a Co^{2+} ion to a Mn^{4+} ion would cost about 0.2 eV according to electrochemical data, the problem is to understand why the introduction of oxygen vacancies would induce such an electron transfer. To address this problem, it is pointed out that oxygen vacancies introduce mobile Mn^{3+} ions, particularly at higher temperatures, and that the elastic energy associated with fluctuations of the occupied *e* orbital at a Mn^{3+} ion may be reduced by the required 0.2 eV by stabilizing other Jahn-Teller near neighbors so that the local distortions can be cooperative. It is therefore suggested that the introduction of oxygen vacancies creates in the second phase a percolating matrix of atomically disordered, intermediate-spin Co^{3+} and Mn^{3+} Jahn-Teller ions.

Demonstration that the two ferromagnetic phases are thermodynamically distinguishable is found in the $M(T)$ curves for samples with $0.02 \leqslant \delta \leqslant 0.05$ that were not quenched. Two ferromagnetic phases were clearly visible, but the degree to which phase segregation reached thermal equilibrium depended on the synthesis conditions. Support for the presence of intermediate-spin Co^{3+} and high-spin Mn^{3+} in the quenched $\delta = 0.05(1)$ sample comes from a $\delta \geqslant 0.05$ sample synthesized at 600 °C. It has a pseudotetragonal ($c/a < \sqrt{2}$) structure that cannot be attributed to a cooperative rotation of the octahedral sites about [001], but can be understood as a static, cooperative orbital ordering at intermediate-spin Co^{3+} and high-spin Mn^{3+} like that in $LaMnO_3$. To deform the lattice symmetry, the static ordering would need to occur in a percolating matrix. In the quenched sample with $\delta = 0.05(1)$, any static orbital ordering would only occur progressively at lower temperatures and be confined to nonpercolating clusters; these clusters would trap out mobile polarons and would suppress the magnetization.

We conclude that the driving force for separation of two distinguishable ferromagnetic phases in the interval $0.02 \leqslant \delta \leqslant 0.05$ is a reduction of the elastic energy associated with local distortive fluctuations at the mobile Mn^{3+} ions introduced by oxygen vacancies; the elastic energy is reduced by the introduction of neighboring Jahn-Teller ions to make the local distortions cooperative, and the additional Jahn-Teller ions are intermediate-spin Co^{3+} and additional Mn^{3+} ions introduced by transfer of an *e* electron from a Co^{2+} ion to a neighboring Mn^{4+} ion.

ACKNOWLEDGMENTS

The authors are grateful to J.-Q. Yan for assistance in the high-pressure oxygen experiments, and to the National Science Foundation and the Robert A. Welch Foundation of Houston, Texas, for financial support.

[1] J. B. Goodenough, Phys. Rev. **100**, 564 (1955).
[2] J. B. Goodenough, J. Phys. Chem. Solids **6**, 287 (1958).
[3] J. B. Goodenough, A. Wold, R. J. Arnott, and N. Menyuk, Phys. Rev. **124**, 373 (1961).
[4] G. Blasse, J. Phys. Chem. Solids **26**, 1969 (1965).
[5] G. T. K. Fey, W. Li, and J. R. Dahn, J. Electrochem. Soc. **141**, 2279 (1994); J. M. Paulsen, C. L. Thomas, and J. R. Dahn, *ibid.* **147**, 861 (2000).
[6] P. A. Joy, Y. B. Khollam, and S. K. Date, Phys. Rev. B **62**, 8608 (2000).
[7] P. A. Joy, Y. B. Khollam, S. N. Patole, and S. K. Date, Mater. Lett. **46**, 261 (2000).
[8] G. H. Jonker, J. Appl. Phys. **37**, 1424 (1966).
[9] M. Pechini, U.S. Patent 3,330,697 (1967).
[10] G. A. Novak and A. A. Colville, Am. Mineral. **74**, 488 (1989).
[11] J. A. Ibers, D. H. Templeton, B. K. Vainshtein, G. E. Bacon, and

K. Lonsdale, in *International Tables for X-ray Crystallography*, edited by C. H. Macgillavry, G. D. Rieck, and K. Lonsdale (Gen. Ed.) (Birmingham, England, 1962), Vol. III, Sec. 3.3, p. 201.

[12] J. B. Goodenough, J.-S. Zhou, and J. Chen, Phys. Rev. B **47**, 5275 (1993).

[13] J.-S. Zhou, H. Q. Yin, and J. B. Goodenough, Phys. Rev. B **63**, 184423 (2001).

[14] J. B. Goodenough, R. I. Dass, and J.-S. Zhou, Solid State Sci. **4**, 297 (2002).

[15] R. I. Dass and J. B. Goodenough, Phys. Rev. B **63**, 064417 (2001); J. B. Goodenough and R. I. Dass, Int. J. Inorg. Mater. **2**, 3 (2000).

[16] S. Yamaguchi, Y. Okimoto, and Y. Tokura, Phys. Rev. B **55**, R8666 (1997).

[17] Despina Louca, J. L. Sarrao, J. D. Thompson, H. Röder, and G. H. Kwei, Phys. Rev. B **60**, 10 378 (1999).

[18] J. B. Goodenough, J. Appl. Phys. **36**, 2342 (1965).

[19] K. R. Poeppelmeier, M. E. Leonowicz, and J. M. Longo, J. Solid State Chem. **44**, 89 (1982).